



Laser-induced blurring of molecular structure information in high harmonic spectroscopy

François Risoud, Camille Lévêque, Marie Labeye, Jérémie Caillat, Alfred Maquet, Pascal Salières, Richard Taïeb, Tahir Shaaran

► To cite this version:

François Risoud, Camille Lévêque, Marie Labeye, Jérémie Caillat, Alfred Maquet, et al.. Laser-induced blurring of molecular structure information in high harmonic spectroscopy. Scientific Reports, 2017, 7, pp.17302. 10.1038/s41598-017-17416-9 . hal-02148237

HAL Id: hal-02148237

<https://hal.science/hal-02148237>

Submitted on 5 Jun 2019

HAL is a multi-disciplinary open access archive for the deposit and dissemination of scientific research documents, whether they are published or not. The documents may come from teaching and research institutions in France or abroad, or from public or private research centers.

L'archive ouverte pluridisciplinaire **HAL**, est destinée au dépôt et à la diffusion de documents scientifiques de niveau recherche, publiés ou non, émanant des établissements d'enseignement et de recherche français ou étrangers, des laboratoires publics ou privés.

SCIENTIFIC REPORTS

OPEN

Laser-induced blurring of molecular structure information in high harmonic spectroscopy

François Risoud¹, Camille Lévêque^{1,2,3}, Marie Labeye¹, Jérémie Caillat¹, Alfred Maquet¹, Pascal Salières⁴, Richard Taïeb¹ & Tahir Shaaran^{4,5}

High harmonic spectroscopy gives access to molecular structure with Angström resolution. Such information is encoded in the destructive interferences occurring between the harmonic emissions from the different parts of the molecule. By solving the time-dependent Schrödinger equation, either numerically or with the molecular strong-field approximation, we show that the electron dynamics in the emission process generally results in a strong spectral smoothing of the interferences, blurring the structural information. However we identify specific generation conditions where they are unaffected. These findings have important consequences for molecular imaging and orbital tomography using high harmonic spectroscopy.

High Harmonic Spectroscopy (HHS) is a powerful technique in which the process of High Harmonic Generation (HHG) is used to probe the structure and dynamics of the generating medium with Angström and attosecond resolution. In HHG, an Electron Wave-Packet (EWP) is prepared by tunnel ionization of the atomic/molecular target gas, it is then accelerated by the strong laser field and finally driven back to the core^{1,2}. In the recombination process, a burst of extreme ultraviolet photons is emitted, encoding a wealth of information on the target. First, the recombination dipole moment imprints the structure of the molecular orbital involved in the emission, under the form of structural interferences³ equivalent to Cohen-Fano interferences in the photo-ionization dipole⁴. The accurate spectral position and shape of the signature of these interferences in the HHG spectrum (amplitude and phase) is the required information for performing molecular imaging³ and orbital quantum tomography^{5–7}. Second, any dynamics occurring in the core during the EWP continuum excursion strongly affects the recombination. For instance, tunnel ionization from different valence orbitals results in interfering channels in the recombination^{8–10}.

However, it is crucial to disentangle the different effects in order to access this rich information^{11–13}. This was generally performed by recording the dependence on the laser parameters (intensity, wavelength), since it was widely accepted that structural interferences do not depend on them¹⁴. This appears clearly in the Quantitative ReScattering theory (QRS)¹⁵ where the harmonic dipole is expressed as the product of the returning EWP, containing all the laser parameters, and the target-specific field-free recombination dipole, only dependent on the EWP energy and recollision direction. Such a factorization has been very successful in predicting and explaining resonant features in the harmonic intensity, e.g., in¹⁶. It was further confirmed by analytic calculations in the case of a model potential¹⁷.

Here, we study the signatures of the electron *dynamics* on the *structural* interference occurring in the harmonic emission from diatomic molecules. Based on Time-dependent Schrödinger Equation (TDSE) calculations resolving the two shortest EWP trajectories for each harmonic, we show that the value of the laser field at recombination plays a crucial role on the shape of the two-center destructive interference. In most cases, the intensity minimum and the associated phase-jump are spread over a broad spectral range resulting in a very smooth behavior, and the phase-jumps for the short and long EWP trajectories are in opposite directions. Furthermore, we identify very peculiar situations for which this phase-jump is very sharp, providing ideal conditions for performing

¹Sorbonne Université, UPMC Univ. Paris 6, CNRS-UMR 7614, Laboratoire de Chimie Physique-Matière et Rayonnement, 4 place Jussieu, 75252, Paris Cedex 05, France. ²Physikalisch-Chemisches Institut, Universität Heidelberg, Im Neuenheimer Feld 229, D-69120, Heidelberg, Germany. ³Department of physics and astronomy, Aarhus University, 8000, Aarhus C, Denmark. ⁴LIDYL, CEA, CNRS, Université Paris-Saclay, CEA-Saclay, 91191, Gif sur Yvette, France. ⁵Max-Planck-Institut für Kernphysik, Saupfercheckweg 1, 69117, Heidelberg, Germany. Correspondence and requests for materials should be addressed to R.T. (email: richard.taieb@upmc.fr)

molecular imaging and quantum tomography. Using the Strong-Field Approximation (SFA) approach¹⁸ modified for molecules^{19,20}, we explain these features by the modification of the saddle-point trajectories induced by the fast phase variation of the recombination dipole. Our findings thus question the *strict* separation between continuum dynamics and recombination advocated, e.g., in QRS, with strong implications for HHS.

We chose to perform our study on a one dimensional (1D) system that contains the essential physics of two-center interference in HHG. This has two advantages: (i) we can easily achieve numerous computations both within the TDSE and the SFA framework, and implement analytical developments; (ii) we avoid additional effects like Coulomb refocusing or EWP spreading that was previously invoked to explain phase smoothing effects^{21,22}. Note that we carried out preliminary 2D computations that are in overall agreement with our 1D results, even though they present extra features, that we plan to address in a forthcoming paper. Our model system represents a diatomic molecule with fixed nuclei, under the single-active electron approximation.

First, we solved the TDSE to simulate the “exact” electron dynamics under the influence of a low-frequency strong laser field. The electron-nuclei interaction is represented by:

$$V(x) = -\frac{1}{2} \left[\frac{1}{\sqrt{a^2 + \left(x + \frac{R}{2}\right)^2}} + \frac{1}{\sqrt{a^2 + \left(x - \frac{R}{2}\right)^2}} \right], \quad (1)$$

where R is the internuclear distance. This is valid for molecules with “heavy” nuclei that exhibit a strong two-center character, such as CO_2 ^{7,23,24}. In order to study the R -dependence of the structural interferences, the regularization parameter a is adapted to maintain the same ground state energy ($-I_p = -0.567 \text{ a.u.} = -15.43 \text{ eV}$) at each considered value of R . The electric field $E(t)$, of amplitude E_L , has a sine-square envelop lasting two optical cycles with frequency ω_L corresponding to a 800-nm Ti:sapphire laser. The carrier-envelope phase is set equal to zero in order to obtain the contributions of only one set of short and long trajectories in the HHG spectrum. The $t \rightarrow \omega$ Fourier transform of the acceleration²⁵ provides the harmonic field. We calibrate the latter with the one calculated for a reference “atom” ($R = 0$ in Eq. 1) with same ionization potential, i.e., we divide the harmonic field calculated for the molecule by the one simulated in the reference atom. This standard procedure in HHS allows removing both the plateau-cutoff shape in the spectrum and the group delay dispersion associated with the attochirp²⁶, in order to evidence the two-center signatures we are interested in. We numerically discriminate the short and long trajectory contributions with an absorber at a distance E_L/ω^2 , using the fact that the short trajectories never go above this limit while the long ones always cross it²⁷.

Figure 1 reports the calibrated harmonic intensity and phase for several internuclear distances between 1.4 and 1.7 a.u., and a laser peak intensity of $2.55 \times 10^{14} \text{ W.cm}^{-2}$. As expected³, the possibility for the electron to recombine on either center results in a destructive two-center interference that appears as a minimum in the spectrum accompanied by a $\approx \pi$ phase-jump. Its position moves to high harmonic orders with decreasing R , since it requires a shorter EWP de Broglie wavelength λ_{dB} ($R \approx \lambda_{dB}/2$). However, we observe in Fig. 1 many remarkable unexpected features: (i) for most R values, the intensity minimum and associated phase-jump are spread over a large spectral range; (ii) the phase-jumps for the short and long trajectories are in opposite directions for high values of R ; (iii) the shape of the interference strongly depends on R . In particular for the long trajectory, at a critical internuclear distance $R_c \approx 1.55 \text{ a.u.}$, the interference becomes extremely destructive at harmonic 41 (H41) with a very steep π phase-jump. For smaller R values, the interference becomes smooth again, but with a change of sign of the phase-jump that now resembles that of the short trajectory. Indeed, the interference is now positioned in the cutoff region ($> \text{H41}$) where the two trajectories coalesce.

Within the QRS, the calibrated emission should be directly proportional to the molecular recombination dipole matrix element. We computed it with the numerically *exact* scattering waves of the potential $V(x)$ and found an excellent agreement *only* at the critical distance R_c and for the long trajectory.

In order to shed light on the above features, we performed a time-frequency analysis of the harmonic dipole using Gabor transforms as in²⁸. We retrieved the emission times of the harmonics for which the destructive interferences occur and found that, at the particular internuclear distance R_c , it corresponds to an almost zero instantaneous electric field for the long trajectory. Furthermore, larger (lower) values of R lead to recollision with a negative (positive) electric field for the long trajectories while it is always positive for the short trajectories. Thus, the sign and shape of the phase-jump seem to be strongly correlated to the instantaneous value of the electric field when the harmonics are emitted.

To further examine the influence of the electric field, we varied the peak laser intensity I_L from 2 to $4 \times 10^{14} \text{ W.cm}^{-2}$ at fixed $R = 1.4 \text{ a.u.}$ and show the results in Fig. 2(a,b). While the position of the destructive interference is relatively independent of I_L (i.e., around H49), the phase-jump behaves similarly when varying R at fixed I_L . We found a critical intensity $I_c = 3.24 \times 10^{14} \text{ W.cm}^{-2}$ for which we observe the inversion of direction with a very sharp π phase-jump. Here again, this value directly corresponds to an instantaneous electric field ≈ 0 when H49 is emitted.

We carried out the same study within the molecular SFA framework, derived following²⁰, the results of which are reported in Fig. 2(c,d). The same conclusions concerning the phase-jump can be drawn, with minor differences on the position of the destructive interference and the laser intensity range. These differences are due to the way the continuum is described in SFA [plane-wave (PW) approximation], and also to the position of the cutoff beyond which harmonics cannot be computed within SFA. These SFA computations reproduce remarkably well the smoothing observed in the TDSE simulations. This evidences that the main origin of the smoothing is not related to Coulomb scattering effects²⁹. A major advantage of the SFA lies in its semi-analytical form. It allows for a semi-classical analysis by searching the saddle-points of the action that determine the main quantum orbits/

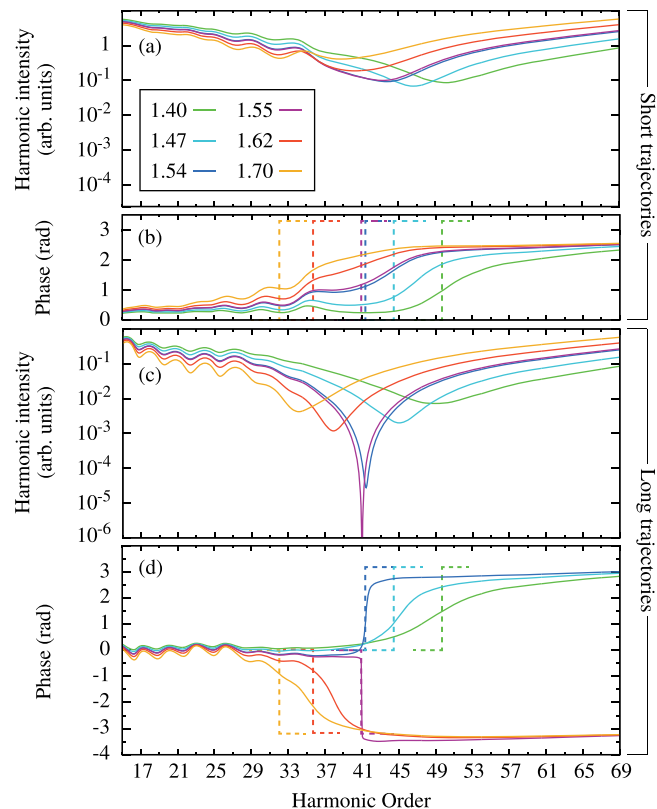


Figure 1. TDSE computations of the short and long trajectory contributions to HHG for a two-cycle laser pulse of $2.55 \times 10^{14} \text{ W.cm}^{-2}$ peak intensity for model molecules of different internuclear distances indicated in a.u. in the legend. We report the harmonic intensity (a) [(c)] and phase (b) [(d)] calibrated by the atomic reference for the short [long] trajectories (solid lines), and the phase of the exact transition dipole matrix element computed numerically for the different internuclear distances [dashed lines in (b) and (d)].

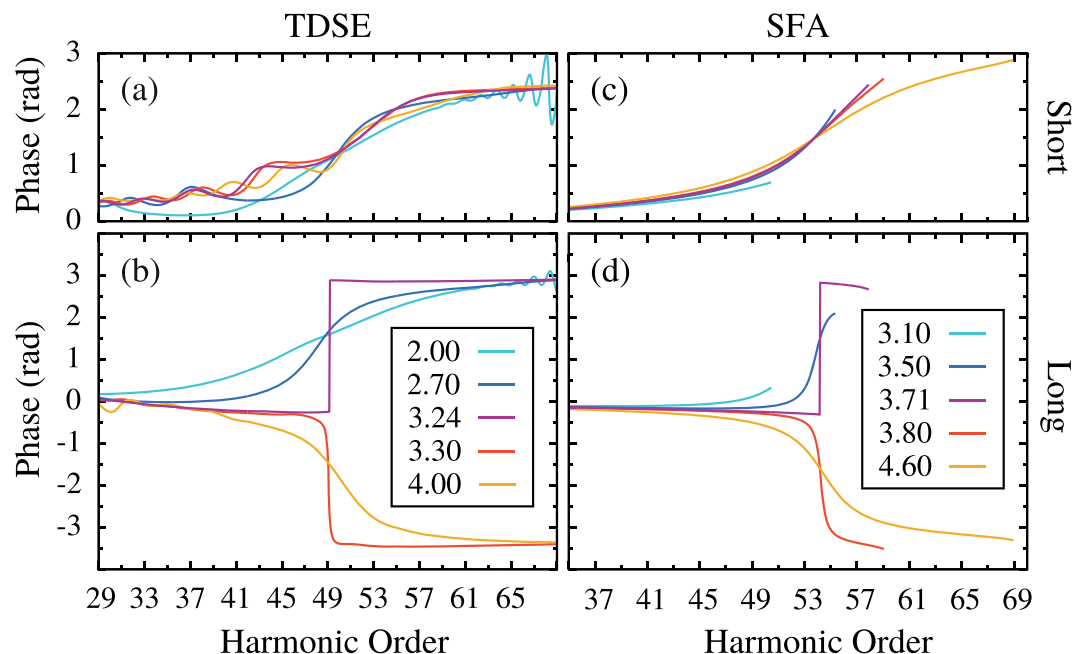


Figure 2. TDSE [Molecular SFA] computations of the harmonic phase of our model molecule ($R = 1.4 \text{ a.u.}$) relative to an atomic reference for the short (a) [(c)] and long trajectories (b) [(d)] at various intensities of a two-cycle laser pulse, indicated in units of $10^{14} \text{ W.cm}^{-2}$ in the legend.

trajectories contributing to HHG^{18,30}. Thus, we performed a Taylor expansion of the stationary solutions for the molecular SFA around the ones for the reference atom to get physical insight into the electron dynamics. Following^{19,20}, we approximate the *symmetric* electronic ground state of a homonuclear diatomic molecule by the sum of two symmetric *atomic* orbitals centered on each nucleus. The PW-recombination and -ionization dipole matrix elements become proportional to $\cos(pR/2)$, with $p = \sqrt{2(\Omega - I_p)}$ the continuum electron momentum associated with each harmonic frequency Ω . By expressing $\cos(pR/2)$ in terms of $\exp[\pm ipR/2]$, the action reads:

$$S_\Omega(p, t, t') = \int_{t'}^t d\tau \left(\frac{[p + A(\tau)]^2}{2} + I_p \right) + \Omega t + \{(-1)^j [p + A(t')] - (-1)^k [p + A(t)]\} \frac{R}{2}, \quad (2)$$

where $j, k \in \{1, 2\}$ label the atomic centers and A is the vector potential associated with the electric field. The first two terms are identical to the atomic SFA while the last two are induced by the fast phase variations of the molecular ionization and recombination dipoles. The saddle-point equations associated with this modified action^{19,20} allow to determine the stationary solutions for the momentum p_{stat} , the ionization and recombination times t'_{stat} and t_{stat} respectively. Compared to their atomic equivalents, we found that p_{stat} is unchanged to first order in the molecular case, while the times t'_{stat} and t_{stat} differ by:

$$\Delta t'_{\text{stat}} = i \frac{(-1)^j R/2}{\sqrt{2I_p}} \text{ and } \Delta t_{\text{stat}} = \frac{(-1)^k R/2}{\sqrt{2(\Omega - I_p)}}, \quad (3)$$

respectively. The physical meaning of these quantities is rather straightforward. They correspond to an increase (decrease) of either the barrier to tunnel through or the path in the continuum, for the electron, whether the nucleus is located at $-R/2$ ($+R/2$) for j or k equal 1 or 2, respectively. As the former is classically forbidden, the change in ionization time is purely imaginary, while the latter, classically allowed, is purely real.

The saddle-point harmonic dipole can then be factorized in the spirit of the QRS but with a modified recombination dipole, which reads to first order:

$$\tilde{d}_{\text{rec}}(p, t) = 2i \mathcal{R}(p) \cos\left(p \frac{R}{2}\right) + 2 \left[E(t) |\Delta t_{\text{stat}}| \frac{\partial \mathcal{R}(p)}{\partial p} + \zeta \right] \sin\left(p \frac{R}{2}\right), \quad (4)$$

where ζ is a constant and $\mathcal{R}(p)$ is proportional to the overlap of the atomic orbitals with the PWs representing the continuum²⁷. One clearly sees that in addition to the “bare” recombination dipole (first term in Eq. (4), here purely imaginary), \tilde{d}_{rec} contains a real valued part varying like $\sin(pR/2)$ and depending on the electric field at recombination time t . We have checked numerically that ζ , which originates from the rigorous handling of the prefactors arising from the saddle-point approximations within SFA, is almost constant and small compared to the other term in the bracket²⁷. It explains why the discontinuous π -jump is observed at an almost but *not exactly* zero electric field at recombination time.

Therefore, (i) \tilde{d}_{rec} is not restricted to the imaginary axis across the HHG spectra and travels in the complex plane, (ii) it does not vanish when the two-center interference term, proportional to $\cos(pR/2)$, is zero, except when the bracket in Eq. (4) is also zero, (iii) it has a real part which is almost proportional to $E(t)$ (ζ is significantly small with respect to the other term in the brackets²⁷) and which value and sign drives the direction and the smoothness of the phase-jump. Thus, $\tilde{d}_{\text{rec}} = 0$ happens *only* when $E(t) \approx 0$ at emission time of H49 of the long trajectory in the conditions of Fig. 2, confirming our findings from both the TDSE and the full molecular SFA simulations.

One should note that, if we neglect ζ in Eq. (4), we recover an expression for \tilde{d}_{rec} close to the one found by including the *ad hoc* dressing of the molecular ground state by the electric field, in the light of ref.³¹. Indeed, in the presence of a laser field, we may approximate the dressed fundamental wave-function as a linear combination:

$$\Phi_0(x, t) \simeq \psi_g(x) + c(t) \psi_u(x), \quad (5)$$

of a symmetric state σ_g (field-free molecular ground-state), sum of two symmetric atomic orbitals centered at $\pm R/2$, and an antisymmetric state σ_u (field-free first excited state), difference of the same two atomic orbitals³². This decomposition is a very good approximation even at short distance R ²⁷.

Within the time-dependent perturbation theory, $c(t)$ depends linearly on the instantaneous electric field $E(t)$, i.e., $c(t) = \chi E(t)$, and we checked, by computing the exact dressed ground-state³³, that this is still valid for fields strength $\approx 10^{14}$ W.cm⁻². Thus, the modified recombination dipole associated with Φ_0 within the PW approximation, becomes:

$$d_{\text{rec}}(p, t) \propto i \cos(pR/2) - \chi E(t) \sin(pR/2), \quad (6)$$

which resembles the expression given in Eq. (4). Thus, the signature of the electron dynamics in \tilde{d}_{rec} was attributed to the manifestation of the dressing of the electronic ground-state.

In practice, the influence of the electron dynamics on the structural interference could be observed by following the phase difference between the short/long trajectory contributions when varying the laser intensity, e.g., by recording the Quantum Path Interferences in the total harmonic dipole^{34,35}.

In summary, we have shown that the electron dynamics in the HHG process may blur the two-center interferences encoding the molecular orbital structure. The value and sign of the driving laser field at recombination become critical in spreading the intensity minimum and associated phase-jump over a large spectral range and

inducing opposite phase-jumps for the short and long trajectories. Except in specific situations, our study demonstrates that the harmonic emission is not entirely proportional to the field-free recombination dipole moment. This raises questions since such factorization is central in HHS, e.g., in the QRS theory. This should be taken into account when comparing the recombination dipole extracted from HHG to the photoionization dipole, or using it for molecular imaging and quantum tomography. Our conclusions could be generalized to other types of structures occurring in the recombination dipole, like shape or autoionization resonances. If narrow enough, the corresponding fast phase variations could modify the electron dynamics and result in a smoother behavior in the harmonic emission. Further studies are in progress to uncover all the implications of the reported findings.

References

1. Corkum P B 1993 *Physical Review Letters* **71**(13) (1994).
2. Schafer, K. J., Yang, B., DiMauro, L. F. & Kulander, K. C. *Physical Review Letters* **70**(11), 1599–1602 (1993).
3. Lein, M., Hay, N., Velotta, R., Marangos, J. P. & Knight, P. L. *Physical Review Letters* **88**(18), 183903 (2002).
4. Cohen, H. D. & Fano, U. *Physical Review* **150**(1), 30–33 (1966).
5. Itatani, J. *et al. Nature* **432**(7019), 867–871 (2004).
6. Haessler, S. *et al. Nature Physics* **6**(3), 200–206 (2010).
7. Vozzi, C. *et al. Nature Physics* **7**(10), 822–826 (2011).
8. McFarland, B. K., Farrell, J. P., Bucksbaum, P. H. & Gühr, M. *Science* **322**(5905), 1232–1235 (2008).
9. Smirnova, O. *et al. Nature* **460**(7258), 972–977 (2009).
10. Diveki, Z. *et al. New J. Phys* **14**, 023062 (2012).
11. Haessler, S., Caillat, J. & Salières, P. *J. Phys. B: At. Mol. Opt. Phys.* **44**, 203001 (2011).
12. Salières, P., Maquet, A., Haessler, S., Caillat, J. & Taeb, R. *Report on Progress in Physics* **75**, 062401 (2012).
13. Diveki, Z. *et al. Chem. Phys.* **414**, 121 (2013).
14. Wörner, H. J., Bertrand, J. B., Hockett, P., Corkum, P. B. & Villeneuve, D. M. *Physical Review Letters* **104**(23), 233904 (2010).
15. Le, A. T., Lucchese, R. R., Tonzani, S., Morishita, T. & Lin, C. D. *Physical Review A* **80**(1), 013401 (2009).
16. Shiner, A. D. *et al. Nature Physics* **7**(6), 464–467 (2011).
17. Frolov, M. V., Manakov, N. L., Sarantseva, T. S. & Starace, A. F. *Physical Review A* **83**(4), 043416 (2011).
18. Lewenstein, M., Balcou, P., Ivanov, M. Y., L’Huillier, A. & Corkum, P. B. *Physical Review A* **49**(3), 2117 (1994).
19. Chirilă, C. C. & Lein, M. *Physical Review A* **73**(2), 023410 (2006).
20. de Morisson Faria Figueira, C. *Physical Review A* **76**(4), 043407 (2007).
21. Chirilă, C. C. & Lein, M. *Physical Review A* **80**(1), 013405 (2009).
22. van der Zwan, E. V. & Lein, M. *Physical Review A* **82**(3), 033405 (2010).
23. Boutu, W. *et al. Nature Physics* **4**(7), 545–549 (2008).
24. Vozzi, C. *et al. Physical Review Letters* **95**(15), 153902 (2005).
25. Burnett, K., Reed, V. C., Cooper, J. & Knight, P. L. *Physical Review A* **45**(5), 3347 (1992).
26. Mairesse, Y. *et al. Science* **302**(5650), 1540–1543 (2003).
27. Risoud F 2016 Theoretical study of attosecond dynamics in atoms and molecules using high-order harmonic generation as a self-probe PhD thesis Université Pierre et Marie Curie-Paris VI.
28. Antoine, P., Piraux, B. & Maquet, A. *Physical Review A* **51**(3), R1750 (1995).
29. Ciappina, M. F., Chirilă, C. C. & Lein, M. *Physical Review A* **75**(4), 043405 (2007).
30. Salières, P. *et al. Science* **292**(5518), 902–905 (2001).
31. Śpiewanowski, M. D. & Madsen, L. B. *Physical Review A* **89**(4), 043407 (2014).
32. Odzak, S. & Milošević, D. B. *Physical Review A* **79**(2), 023414 (2009).
33. Maier, C. H., Cederbaum, L. S. & Domcke, W. *Journal of Physics B: Atomic and Molecular Physics* **13**(4), L119 (1980).
34. Zaïr, A. *et al. Physical Review Letters* **100**(14), 143902 (2008).
35. Zaïr, A. *et al. Chemical Physics* **414**, 184–191 (2013).

Acknowledgements

We thank T. Auguste and T. Ruchon for fruitful discussions. We acknowledge financial support from the LABEX Plas@Par-ANR-11-IDEX-0004-02 and ANR-10-LABX-0039-PALM, the programs ANR11-EQPX0005-ATTOLAB, ANR-15-CE30-0001-01-CIMBAAD and the European Networks ITN-ATTOFEL and ITN-MEDEA.

Author Contributions

P.S. and T.S. initiated the study. T.S., F.R., C.L. and M.L. performed the calculations and computations under the supervision of P.S., A.M., J.C. and R.T. The manuscript was cowritten by F.R., P.S., J.C. and R.T. and was reviewed by all authors.

Additional Information

Competing Interests: The authors declare that they have no competing interests.

Publisher's note: Springer Nature remains neutral with regard to jurisdictional claims in published maps and institutional affiliations.



Open Access This article is licensed under a Creative Commons Attribution 4.0 International License, which permits use, sharing, adaptation, distribution and reproduction in any medium or format, as long as you give appropriate credit to the original author(s) and the source, provide a link to the Creative Commons license, and indicate if changes were made. The images or other third party material in this article are included in the article's Creative Commons license, unless indicated otherwise in a credit line to the material. If material is not included in the article's Creative Commons license and your intended use is not permitted by statutory regulation or exceeds the permitted use, you will need to obtain permission directly from the copyright holder. To view a copy of this license, visit <http://creativecommons.org/licenses/by/4.0/>.